

## Spectral reflectance of carbonate minerals in the visible and near infrared (0.35–2.55 microns): calcite, aragonite, and dolomite

SUSAN J. GAFFEY<sup>1</sup>

*Planetary Geosciences Division  
Hawaii Institute of Geophysics  
University of Hawaii at Manoa, Honolulu, Hawaii 96822*

### Abstract

Spectral reflectance in the visible and near infrared portion of the spectrum (0.35 to 2.55  $\mu\text{m}$ ) offers a rapid, inexpensive, non-destructive technique for determining mineralogy and providing some information on the minor element chemistry of the hard-to-discriminate carbonate minerals. It can, in one step, provide information previously obtainable only by the combined application of two or more techniques, and can provide a useful complement to existing mineralogical and petrographic methods for study of carbonates. Calcite, aragonite, and dolomite all have at least 7 absorption features in the 1.60 to 2.55  $\mu\text{m}$  region due to vibrational processes of the carbonate ion. Positions and widths of these bands are diagnostic of mineralogy and can be used to identify these three common minerals even when an absorption band due to small amounts of water present in fluid inclusions masks features near 1.9  $\mu\text{m}$ . Broad double bands near 1.2  $\mu\text{m}$  in calcite and dolomite spectra indicate the presence of  $\text{Fe}^{2+}$ . The shapes and positions of these bands, if present, can aid in identification of calcites and dolomites. Spectra may be obtained from samples in any form, including powders, sands, and broken, sawed, or polished rock surfaces.

### Introduction

Spectral reflectance in the visible and near infrared (0.35 to 2.55  $\mu\text{m}$ ) offers a rapid, inexpensive, nondestructive technique for determining the mineralogy and obtaining some information on the minor element chemistry of the hard-to-discriminate carbonate minerals, and can, in one step, provide information previously obtainable only by the combined application of two or more analytical techniques. The technique has been used for more than a decade to study pyroxenes and olivines, and to a lesser extent feldspars and other mineral groups (e.g., Adams, 1974; Burns, 1970; Dowty and Clark, 1973). Previous work has shown that reflectance spectra of carbonate minerals in the visible (VIS) and near-infrared (NIR) show a variety of features which are caused by multiphonon absorptions of the fundamental internal and lattice vibrational modes of the carbonate radical, and by electronic processes in the unfilled *d*-shells of transition metal cations, if present (Adams, 1974; Hexter, 1958; Hunt and Salisbury, 1971). However, as yet no systematic attempt has been made to relate these spectral features to the mineralogical and chemical composition of carbonate rocks and minerals.

The purpose of this work was to make a detailed study of the spectral properties of well-characterized carbonate mineral and rock samples, and to determine what types of chemical and mineralogical information could be ob-

tained from their reflectance spectra. A previous paper (Gaffey, 1985) briefly summarized data on positions of carbonate and  $\text{Fe}^{2+}$  bands in spectra of carbonate minerals. The present paper deals with the spectra of the three most common carbonate minerals (calcite, aragonite, and dolomite) in detail, and describes changes in spectral properties which reflect differences in mineralogy. Effects of particle size on spectral properties are also discussed. Spectral properties of other less common anhydrous carbonate minerals will be dealt with in a second paper, and changes in spectral properties associated with changes in chemical composition of some common calcite group minerals will be dealt with quantitatively in a third paper.

### Methods

Samples used in this study are listed in Table 1. Mineralogy of all samples was verified by X-ray diffraction. Chemical data on samples were obtained using X-ray fluorescence and AA. Samples for which sufficient material was available were analyzed for CaO, MgO, FeO, and MnO by X-ray fluorescence on fused glass discs, following the procedures of Norrish and Hutton (1969).  $\text{CO}_2$  content was calculated assuming stoichiometry and absence of water. Atomic absorption was done using a Perkin-Elmer 603 Atomic Absorption Spectrophotometer. All samples were washed three times in distilled, deionized water. Two tenths of a gram of sample was dissolved using concentrated HCl diluted to 10% and distilled, deionized water was added to give 100 ml of solution. A like amount of ultrapure  $\text{CaCO}_3$  was added to standards. Each analysis was performed at least twice. Reproducibility for Fe in dolomites was 2.5% or better.

Spectra for calibration work were obtained from mineral sam-

<sup>1</sup> Present address: Department of Geology, Rensselaer Polytechnic Institute, Troy, New York 12181.

Table 1. Numbers and localities of samples used in this study

Calcites	
1507	Pine Pt., Canada <sup>1</sup>
1530	Ultrapur CaCO <sub>3</sub> powder, Alfa Division, Ventron <sup>2</sup>
1531	Iceland spar, Chihuahua Mexico <sup>3</sup>
1542	Egremont, England <sup>4</sup>
6506	Prairie du Chien Fm., Allamakee Co., Iowa
10519	Mexico <sup>5</sup>
Aragonites	
10530	Bilin, Bohemia <sup>4</sup>
10525A	Molina de Aragon, Spain
10524	Spain
Dolomites	
2501	Styria, Austria <sup>6</sup>
5501	Gilman, Colorado <sup>7</sup>
6503	Bahia, Brazil <sup>8</sup>
6509	Deep Springs, Inyo County, Calif. <sup>9</sup>
6510b	Bamle, Telemark, Norway <sup>9</sup>
6514	Binnenthal, Valais, Switzerland <sup>10</sup>

1. Smithsonian Inst. #122283; 2. Alfa Div., Ventron, 152 Andover St., Danvers, Ma.; 3. Wards Natural Science Establishment; 4. Geology Dept., Univ. of Iowa, Iowa City, Iowa; 5. Rainbow Collection, Honolulu, HI.; 6. Smithsonian Inst. #B9764; 7. Smithsonian Inst. #R15143; 8. Smithsonian Inst. #103165; 9. Minerals Unlimited, Ridgecrest, Calif.; 10. British Museum #1912,133.

ples ground or crushed by hand in a ceramic mortar and pestle. Because most scattering of light occurs at crystal-air interfaces, light travels farther in coarse-grained samples and non-porous rocks than in fine powders before being reflected back to the detector. Larger particle sizes increase the optical path length and therefore the intensity of absorption features (see below). However, the low optical density of carbonates can result in light passing through the sample and reflections being obtained from the sample holder as well as the sample. Thus care had to be exercised in selection of particle size range and sample holder geometry. If sufficient material was available (a few grams) ground samples were wet-sieved to give a fraction with particles ranging from 90 to 355  $\mu\text{m}$  in diameter. When smaller amounts of material were available, finer particle sizes were included in the sample to increase scattering and ensure that all light reaching the detector had interacted only with the sample and not with the sample holder. Calcite sample 1531 was ground and wet-sieved into different size-fractions to study variations in spectral properties with grain size. Spectra of whole rock samples were obtained from broken, sawed, or polished surfaces.

The spectrogoniometer used was designed and built at the University of Hawaii, and is described in detail by Clark (1981a), McCord et al. (1981), and Singer (1981). The instrument is designed to measure bidirectional reflectance. A collimated light source and viewing mirrors are mounted on rocker arms to permit variations in viewing geometry. The VIS and NIR portions of the spectrum are measured by continuously spinning circular variable filters (CVFs). Filters and detectors (an S1 photomultiplier tube for the VIS and an indium antimonide detector for the NIR) are cooled to liquid nitrogen temperatures. Wavelength calibration is checked at the beginning of each day with a narrow band pass filter. Spectral resolution is about 1.5% throughout the spectral range.

Samples were viewed at a phase angle of 10°, with either the light source or the mirrors at the vertical. This viewing geometry was chosen to maximize intensities of absorption bands while avoiding backscatter effects. Each spectrum is an average of several separate observations. The NIR spectra are averages of 5

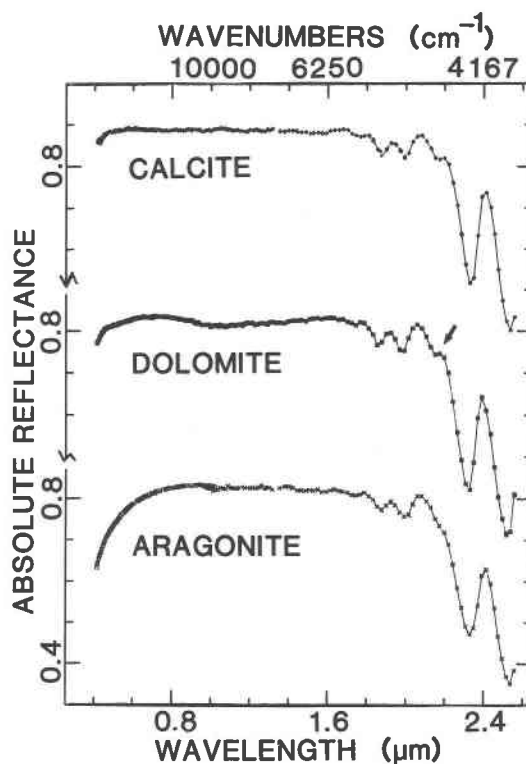


Fig. 1. Spectra of the three most common rock-forming carbonate minerals. Arrow indicates local minimum in curve which occurs in the same region of the spectrum in calcite spectra, but not in aragonite spectra, due to smaller separation between centers and greater degree of overlap between bands 3 and 4 in aragonite spectra. Dots are data points; lines connect data points to outline bands.

runs, each run consisting of two complete revolutions of the CVF. The VIS spectra are averages of 3 runs each with 10 revolutions per run. Since carbonate samples are generally bright, long integrating times were unnecessary. Errors, plus or minus one standard deviation of the mean, are generally less than 0.2%.

Halon, a fluorocarbon manufactured by Allied Chemical Corporation, which is close to a perfect diffuse reflector in this region (Venable et al., 1976; Weidner and Hsia, 1981) was used as a standard. The spectrum of the standard was measured before and after each sample spectrum. Sample spectra were ratioed to the Halon spectrum, and a correction was made for the fact that Halon has a weak absorption feature near 2.15  $\mu\text{m}$ , giving a result felt to be within a few percent of absolute bidirectional reflectance (Singer, 1981). Vertical axes of spectra are thus labeled "absolute reflectance." Where spectra have been offset vertically, e.g., by continuum removal, or to create plots which allow two or more spectra to be compared in a single plot, vertical axes are labeled "relative reflectance."

Data were reduced using spectrum processing routines described by Clark (1980). Precise band positions, intensities, and widths were determined using the GFIT (Gaussian Fitting Program) routine which was adapted from the work of Kaper et al. (1966) and is described by Clark (1981b) and Farr et al. (1980). This routine fits Gaussian functions to all absorption bands simultaneously, quantitatively specifying their positions, widths, and depths.

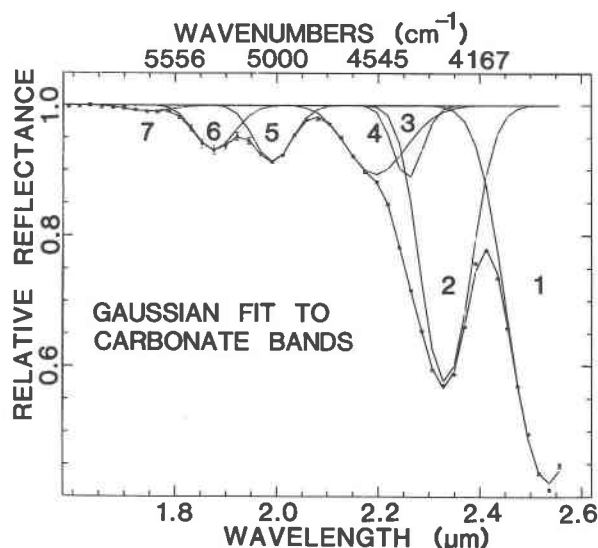


Fig. 2. Data points with error bars (dots) and fit (lines) to these data using the gaussian fitting routine (GFIT). The lines show both the individual gaussians fit to the data (numbered 1 to 7) and the fit curve which is the sum of these gaussians.

## Results

### Carbonate bands

Figure 1 shows typical spectra of calcite, aragonite, and dolomite. The crystal structure and chemical composition of these minerals are discussed in detail in the review articles by Goldsmith (1983), Reeder (1983), and Speer (1983). Spectra of powders of carbonate minerals containing no transition metal cations are nearly straight lines near unity reflectance at wavelengths shorter than  $1.6 \mu\text{m}$ . At the shortest wavelengths ( $<0.7 \mu\text{m}$ ) the aragonite spectrum shows a marked drop-off towards the ultraviolet. The drop-off in the dolomite spectrum is less pronounced, and it is nearly absent in the calcite spectrum. At wavelengths  $>1.6 \mu\text{m}$  there is a series of absorption features which increase in intensity with increasing wavelength. These bands are due to vibrational processes of the carbonate radical (Hexter, 1958; Hunt and Salisbury, 1971; Matossi, 1928; Schroeder et al., 1962).

*Gaussian analysis.* Because carbonate spectra are approximately straight lines at short wavelengths, a straight line continuum was selected and removed from the spectrum by division, leaving only the absorption bands. Gaussian curves were then fit in energy space with band intensities on a log scale. Several (4 or more) continua with slightly different slopes were divided into each spectrum, and the result fitted. One of these fits is shown in Figure 2. The best fit was selected on the basis of the errors (residual errors for each data point, errors in band position for each band, and errors in the integrated intensities of the gaussians, i.e., the width times the height) and examination of plots of the data and fits. Figure 3 shows an example with the original data and the different continua tried. The continuum which gave the best fit is indicated

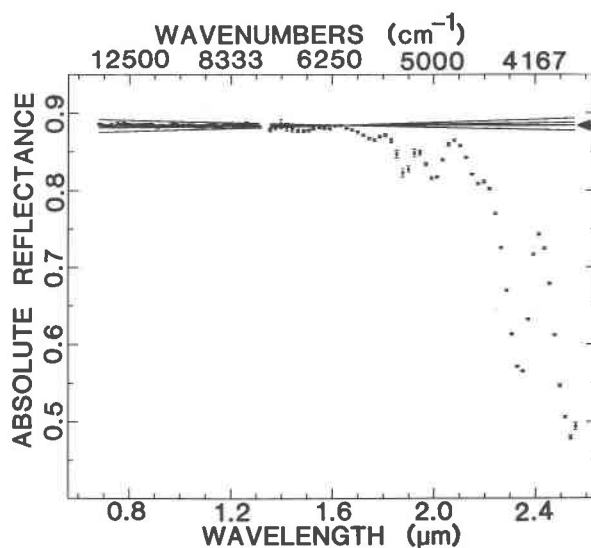


Fig. 3. Plot of the original data (dots) and the different continua divided out of the data for gaussian analyses. Arrow indicates continuum which gave the best fit.

in Figure 3 and, as was generally the case, coincides quite closely with the straight-line portion of the spectrum below  $1.6 \mu\text{m}$ . Slopes of continua varied somewhat from one mineral sample to another, and showed no correlation with mineral type. All were close to horizontal.

For a single mineral spectrum, slightly different band positions were obtained from fits for continua with different slopes. However, differences in band position due

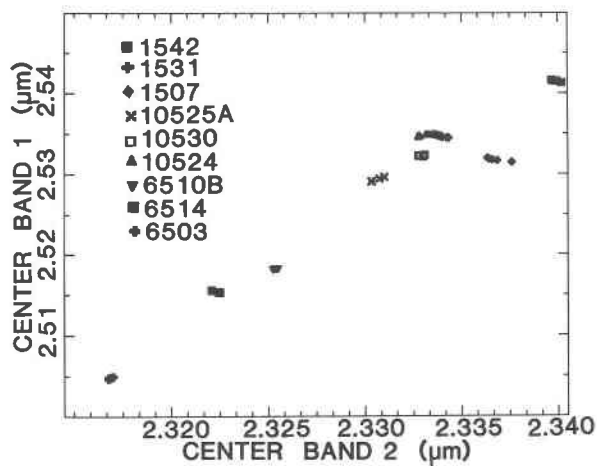


Fig. 4. Positions of the centers of band 1 plotted vs. the positions of the centers of band 2 for all the fits achieved for nine different spectra (3 aragonites, 3 dolomites, and 3 calcites). Each dot represents a band center determined for one continuum. There are between four and nine points plotted for each sample, depending on the number of continua for which a fit could be achieved. Samples 1542, 1531, and 1507 are calcites, 10525a, 10530, and 10524 are aragonites, and 6510b, 6514, and 6503 (the last two represented by the squares and crosses in the lower left-hand portion of the plot) are dolomites.

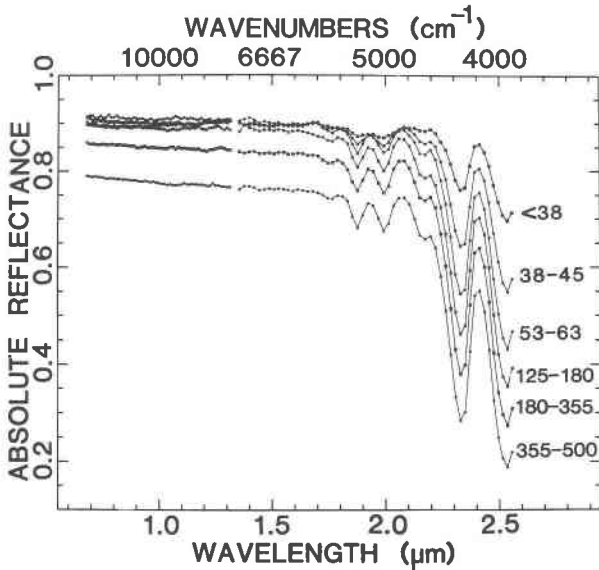


Fig. 5. Spectra of different grain-size fractions obtained by grinding and sieving an Iceland spar sample (1531). Dots—data points; lines connect data points to outline bands. Size fraction given in  $\mu\text{m}$ .

to variations in continuum slope are generally much smaller than differences in band position between different samples of the same mineralogy, and are significantly smaller than differences in band positions due to differences in mineralogy (compare Fig. 4 to Fig. 9). Figure 4 shows positions of centers of band 1 plotted vs. the positions of centers of band 2 for all fits achieved for 9 different spectra—3 aragonites, 3 dolomites, and 3 cal-

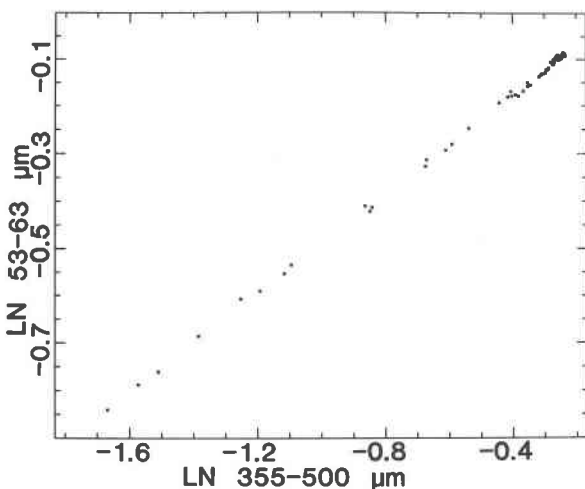


Fig. 6. Natural log of the reflectances at each wavelength in the spectrum of the 53–63  $\mu\text{m}$  fraction plotted as a function of the natural log of the reflectances in the 355–500  $\mu\text{m}$  fraction of sample 1531. These fall approximately along a straight line, indicating absorption features due to carbonate bands follow Lambert's law.

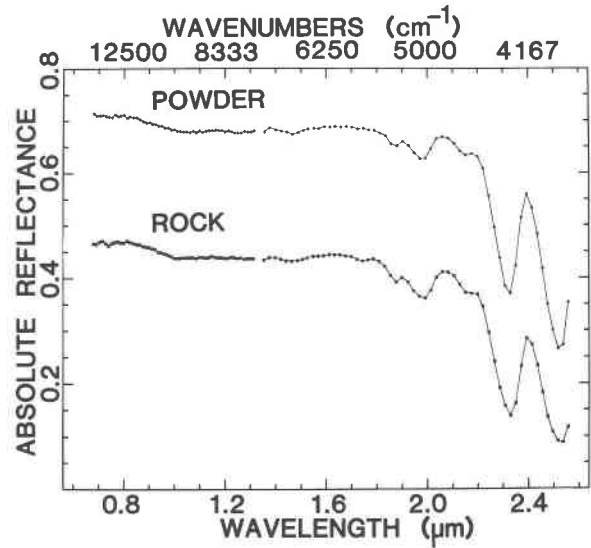


Fig. 7. Two spectra obtained from the same sample (6509) in powdered and whole form.

ites. Each dot represents a band center determined for one continuum. There are between 4 and 9 points plotted for each sample, depending on the number of continua for which a fit was achieved.

*Effects of particle size and packing.* An objection frequently raised to the use of reflectance spectra in this region is that variations in particle size will cause changes in relative intensity, position and shape of bands unrelated to mineralogy (as is the case in the MIR, see below). Figure 5 shows the effects of grain size on the spectral properties of calcite sample 1531. These spectra show that the only spectral parameters which vary with grain size are overall brightness of the sample and absolute band intensity; number of bands, band positions and widths, and relative band intensities (ratios of the intensity of a given band to that of the other bands in the same spectrum) do not change. Gaussian analyses support this observation. With the exception of band 5, gaussian analyses show no systematic changes in band width or relative band depths. For the strongest bands (1 through 3) the variations between relative band intensities and widths are  $<15\%$ . For the weaker bands the variations are larger, but are not systematic, and are of the same order as variations attributable to differences in continuum slope. Band 5 is the exception and does show a systematic increase in width and relative depth with decrease in particle size, relative band depth and width being 50% greater in the spectrum of the  $<38 \mu\text{m}$  fraction than in that of the 355–500  $\mu\text{m}$  fraction. The greatest difference in the width of band 5 ( $\sim 30\%$ ) for the spectra shown in Figure 5 occurs between the spectra of the  $<38 \mu\text{m}$  and the 45–53  $\mu\text{m}$  fractions. This is probably due to an increase in the amount of water adsorbed on the surfaces of fine particles in the smallest size fractions (see discussion of water bands below).

Fitting of curves was done with a vertical scale of the logarithm of the intensity. This is in accordance with Lam-

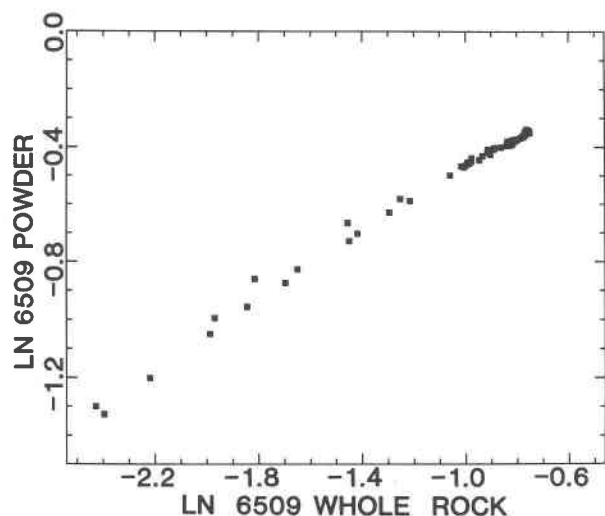


Fig. 8. Ln-ln plot like that in Fig. 6 of the two dolomite spectra shown in Fig. 7. The points fall approximately along a straight line, indicating the Lambert's Law model can be used for spectra of rock samples as well as for powders.

bert's Law, which states that if  $I_0$  is the original light intensity and  $I$  the intensity of the light after passing through a thickness  $x$  of a mineral whose absorption coefficient is  $k$ , then

$$I = I_0 e^{-kx}$$

Figure 6 is a plot of the natural log of the reflectances at each wavelength in the spectrum of the 53–64  $\mu\text{m}$  fraction plotted against the natural log of the reflectances of the 355–500  $\mu\text{m}$  fraction of sample 1531, two of the spectra shown in Figure 5. The ln-ln plots of these two particle size fractions as well as all other combinations tried, fall along a straight line, to a very good first approximation. This demonstrates that absorption of light by carbonate minerals approximates that predicted by Lambert's Law, and lends support to the use of this particular model in studying absorption features in carbonates. An objection frequently raised to the use of reflectance spectra in this region is that they do not adhere to Kubelka-Munk theory. The more commonly employed Kubelka-Munk model is strictly applicable only to weakly absorbing materials; strong absorbers show marked deviation from the theory (Wendlandt and Hecht, 1966). Clark and Roush (1984) found that this marked deviation from the predicted linear trend of the remission function of Kubelka-Munk theory occurs below reflectance values of  $\sim 64\%$ , and summarize other problems which result from attempts to apply Kubelka-Munk theory to geological data.

Another factor affecting both the absolute intensities of spectral features, and the overall brightness, or albedo, of the samples, is porosity or packing of the sample. Figure 7 shows two spectra of the same sample, in powdered and whole form. The sample is a coarse-grained, dense dolomite (sample #6509). Only intensity of bands and overall brightness of the spectra are affected. The number of

Table 2. Band positions determined using gaussian analysis. In  $\mu\text{m}$

	$\mu\text{m}$						
	Band Number						
	1	2	3	4	5	6	7
Sample #							
Calcites							
1507	2.532	2.337	2.265	2.171	1.995	1.882	1.756
1530	2.530	2.334	2.254	2.169	1.995	1.881	1.762
1531	2.535	2.333	2.261	2.167	1.991	1.876	1.763
1542	2.541	2.340	2.272	2.179	1.998	1.885	1.758
6506	2.535	2.334	2.263	2.174	1.974	1.871	1.753
10519	2.533	2.334	2.259	2.169	1.979	1.875	1.770
Dolomites							
2501	2.508	2.313	2.234	2.155	1.971	1.872	
5501	2.513	2.323	2.244	2.150	1.975	1.882	
6503	2.505	2.312	2.235	2.157	1.971	1.853	1.735
6509	2.516	2.320	2.248	2.165	1.974	1.869	
6510b	2.518	2.322	2.247	2.170	1.977	1.867	
6514	2.516	2.319	2.244	2.165	1.979	1.862	1.740
Aragonites							
10524	2.535	2.331	2.257	2.195	1.992	1.877	1.748
10525A	2.529	2.328	2.254	2.186	1.990	1.873	1.744
10530	2.532	2.332	2.258	2.201	1.993	1.874	1.737

features, their form, positions, and relative intensities are not. A ln-ln plot of these two spectra is shown in Figure 8. Here the points also fall approximately along a straight line. Thus Lambert's Law appears to describe absorption features in carbonates, regardless of the form of the sample (i.e., powder, rock, etc.).

*Mineralogical variations.* Positions of 7 carbonate bands in the NIR determined in this study are given in Table 2. Bands are labeled in order of decreasing intensity, the strong 2.5  $\mu\text{m}$  band being band 1. In some spectra the broad, weak band 7 appears to be composed of two bands. However, the resolution in this portion of the spectrum on our instrument made discrimination of these two bands possible in only a few of the spectra, so the two bands

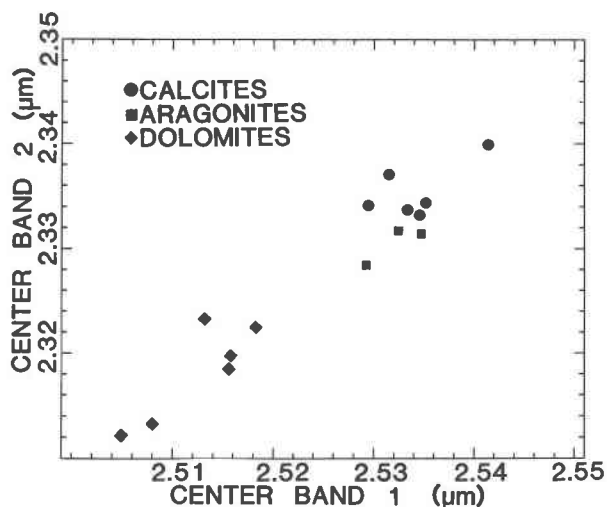


Fig. 9. Position of center of band 2 plotted against position of center of band 1 for each sample.

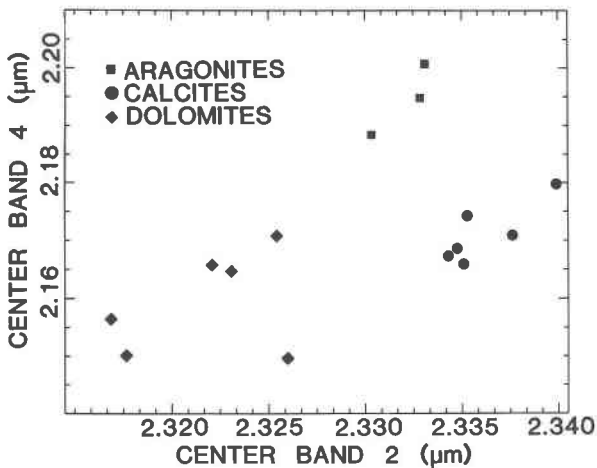


Fig. 10. Position of band centers for bands 2 and 4 for each sample. Here the 3 mineral types separate into three distinct groups according to mineralogy.

were fit as one. In spectra of some other samples, most notably ferroan dolomites, band 7 was too weak for its position to be determined using the GFIT routine, and no band positions are reported for band 7 in these spectra.

In general, all of the bands in dolomite spectra are centered at shorter wavelengths than the equivalent bands in calcite spectra (see Table 2), although there is some overlap in the case of band 4. Band 5 in two of the calcite spectra (samples 10519 and 6506) occurs at the shorter wavelengths typical of the spectra of dolomites. The positions obtained for band 5 in these two spectra using GFIT are  $\sim 0.02 \mu\text{m}$  lower than those of the other calcite spectra. Reflectance spectra are extremely sensitive to the presence of water, which has a strong absorption feature at  $1.9 \mu\text{m}$  (Aines and Rossman, 1984; Hunt, 1977; Hunt and Salisbury, 1971). In the course of the present study it was found that water, most probably in the form of

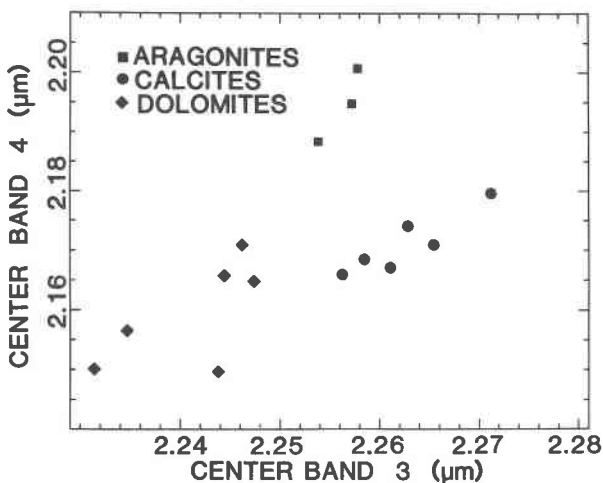


Fig. 11. Positions of centers of band 4 plotted against those for band 3 for each sample.

Table 3. Widths of carbonate bands in  $\mu\text{m}^{-1}$

Sample #	Band Number						
	1	2	3	4	5	6	7
Calcites							
1507	0.0223	0.0154	0.0149	0.0170	0.0183	0.0190	0.0256
1530	0.0228	0.0168	0.0121	0.0288	0.0278	0.0229	0.0255
1531	0.0233	0.0157	0.0139	0.0210	0.0195	0.0206	0.0271
1542	0.0255	0.0161	0.0142	0.0252	0.0223	0.0193	0.0430
6506	0.0237	0.0164	0.0136	0.0268	0.0330	0.0246	0.0305
10519	0.0232	0.0163	0.0144	0.0235	0.0305	0.0241	0.0425
Dolomites							
2501	0.0218	0.0191	0.0138	0.0266	0.0322	0.0188	0.0178
5501	0.0223	0.0178	0.0109	0.0188	0.0233	0.0241	0.0241
6503	0.0221	0.0201	0.0099	0.0306	0.0341	0.0261	0.0330
6509	0.0208	0.0173	0.0104	0.0265	0.0218	0.0222	0.0222
6510b	0.0226	0.0187	0.0113	0.0310	0.0236	0.0226	0.0226
6514	0.0228	0.0186	0.0110	0.0281	0.0206	0.0234	0.0395
Aragonites							
10524	0.0243	0.0192	0.0130	0.0278	0.0218	0.0258	0.0351
10525A	0.0234	0.0197	0.0126	0.0256	0.0275	0.0240	0.0280
10530	0.0247	0.0196	0.0128	0.0296	0.0211	0.0252	0.0357

fluid inclusions, is nearly ubiquitous in carbonate minerals and rocks, although if the amount of water present is small, the water bands are weak and their presence may not become apparent until gaussian analysis is attempted. The spectra of both these samples indicate minor amounts of water are present (a few hundredths of a percent by weight as determined by heating the sample to  $1000^\circ\text{C}$  for  $\frac{1}{2}$  hour and measuring the amount of water evolved). The strong absorption feature due to liquid water which occurs in the  $1.9 \mu\text{m}$  region probably causes the apparent shift to shorter wavelengths of the measured band positions in these two sample spectra. In spectra of all the dolomites studied except sample #5501, band 6 occurs at shorter wavelengths than the same band in calcite spectra. The limited data available indicate that band 7, like the other bands, occurs at shorter wavelengths than its calcite counterpart.

Aragonite bands may occur at the same, shorter, or longer wavelengths than equivalent bands in calcite spectra (see Table 2 and Figs. 9 to 11). While bands 1, 5 and 6 in aragonite spectra occur at the same or slightly shorter wavelengths than equivalent bands in calcite spectra, bands 2, 3 and 7 all occur at significantly shorter wavelengths, and band 4 occurs at longer wavelengths than its counterpart in calcite spectra.

Differences in carbonate band positions in dolomite spectra can be correlated with differences in iron content. For example, data in Table 2 for dolomites 6509 containing 0.04 wt.% Fe, and 6510b containing 2.7 wt.% Fe as determined by AA, show that carbonate bands 1 and 2 tend to be shifted to longer wavelengths with increased Fe content. Such chemical variations probably account for the large scatter in band positions for dolomite spectra.

Band widths also vary with mineralogy. Table 3 shows band widths determined by gaussian analysis of the spectra of the three common mineral types. These widths are given in inverse microns ( $\mu\text{m}^{-1}$ ) rather than microns be-

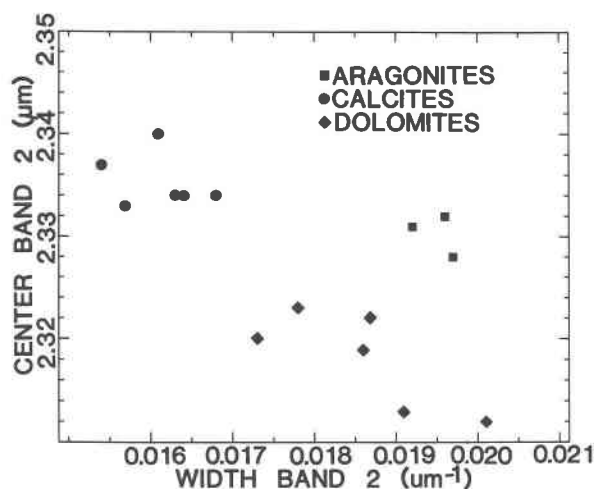


Fig. 12. Positions of centers of band 2 in microns plotted against the widths of band 2 in  $\mu\text{m}^{-1}$  for all samples.

cause the model used here assumes the absorptions represent a Gaussian distribution of energies around a central value (Farr et al., 1980). Since energy is inversely proportional to wavelength, bands are not symmetric in wavelength space. These data indicate band 1 is narrower in dolomite than in aragonite and calcite spectra, although there is some overlap in values for calcites and dolomites. In general these data show band 2 to be widest in aragonite spectra, band 3 to be widest in calcite spectra and narrowest in dolomite spectra, and no clear trends in widths of band 4. The data do not permit generalizations about trends in widths of bands 5 and 6 because minor amounts of water in a sample can increase the apparent width of

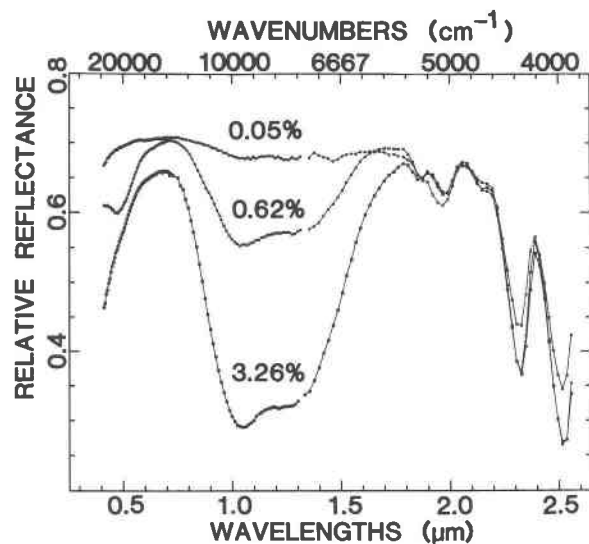


Fig. 13. Spectra of three dolomite samples with different iron contents (given as weight percent FeO) determined by X-ray fluorescence. Dots—data points, connected by lines to outline bands. Feature near  $0.45 \mu\text{m}$  in second spectrum due to  $\text{Fe}^{3+}$  in Fe oxides formed by weathering.

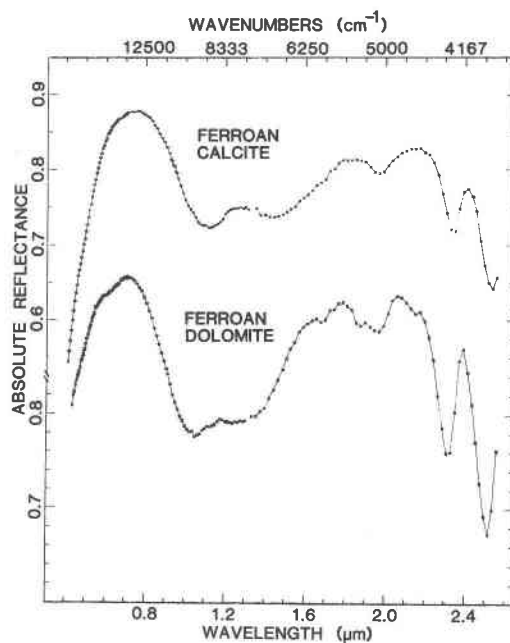


Fig. 14. Spectra of ferroan calcite (upper spectrum) and ferroan dolomite (lower spectrum) showing difference in shape and position of  $\text{Fe}^{2+}$  bands. Dots—data points, connected by lines to outline absorption bands.

these bands (for example, compare widths of band 5 for 10519 and 6506 to those for 1507, 1531, and 1542 in Table 3).

In general dolomite spectra show much greater variation in band widths than aragonite and calcite spectra. This might be related to stoichiometry or lack thereof in dolomite composition, to differences in  $\text{Fe}^{2+}$  and  $\text{Mn}^{2+}$  content, or to the occurrence of zones of different chemical composition within dolomite crystals.

Figures 9, 10 and 11 are plots of some of the data in Table 2. Band-band plots provide a convenient way of displaying such data, and of highlighting differences in spectral properties. These figures illustrate the trends in band position discussed above and show how positions of the first four carbonate bands vary with mineralogy. Note that the samples fall into three distinct groups according to mineralogy.

Band widths may also be used to distinguish carbonate minerals from each other. Figure 12 shows the center of band 2 plotted vs. the width of band 2 for each sample. The samples again fall into three groups of different mineralogy.

#### Iron bands

Although variations in spectral properties with variations in chemical composition will be dealt with in detail elsewhere, a brief discussion of absorption features due to the presence of ferrous iron in calcite and dolomite is presented here, as these features can aid in mineral identification. A broad band near  $1.2\text{--}1.3 \mu\text{m}$  occurs in some calcite spectra, and in all dolomite spectra, but is absent



from all aragonite spectra measured in the course of this study. Both  $\text{Fe}^{2+}$  and  $\text{Cu}^{2+}$  can produce broad absorption features near  $1.0 \mu\text{m}$  (Holmes and McClure, 1957; Bjerrum et al., 1954; Ballhausen, 1962; and others). We can infer that this broad feature is caused by  $\text{Fe}^{2+}$  because:

1. The common occurrence of  $\text{Fe}^{2+}$  substituting for  $\text{Ca}^{2+}$  and  $\text{Mg}^{2+}$  in calcites and dolomites (Deer et al., 1962; Lippmann, 1973; Reeder, 1983; and others) makes it the most likely transition metal ion to result in such a commonly occurring absorption band.

2. Increase in intensity of this broad band is positively correlated with increasing iron content in dolomites (see Fig. 13) and calcites.

Absorption bands in calcite and dolomite spectra due to  $\text{Fe}^{2+}$  differ in position and shape. Figure 14 shows the  $\text{Fe}^{2+}$  feature in the calcite spectrum is a broad double band centered near  $1.3 \mu\text{m}$ , while that in the dolomite spectrum is centered at  $\sim 1.2 \mu\text{m}$ . Although the  $\text{Fe}^{2+}$  features in both spectra are composed of at least two broad bands, the splitting between the bands is much more pronounced in the calcite spectrum.

Intensities of bands due to transition metal ions are, like intensities of features due to vibrational processes of the carbonate radical, affected by particle size and packing. However, intensities of features due to transition metal cations are affected by concentration of the cation in the crystal as well. Figure 13 shows spectra of three dolomites containing different concentrations of iron. The carbonate bands in all three spectra are of about the same intensity, indicating that the particle size distributions of the powdered samples are comparable. The iron bands, however, are of different intensities, intensity increasing with increasing  $\text{Fe}^{2+}$  concentration.

## Discussion

### *Applicability of technique to geologic problems*

Considerable work has been done with transmission and reflection spectra of carbonates in the mid-infrared (MIR) ( $5\text{--}15 \mu\text{m}$ ) region where absorption features caused by the fundamental vibrational modes of the carbonate ion occur. Spectra in this region have been used to study the structure of carbonate minerals (Adler and Kerr, 1962, 1963a,b; Gatehouse et al., 1958; Hexter and Dows, 1956; Scheetz and White, 1977; Schroeder et al., 1962; Weir and Lippincott, 1961; and many others), and some efforts have been made to use spectra in this region for mineralogical and petrographic studies of carbonates (Adler and Kerr, 1962; Chester and Elderfield, 1966, 1967; Farmer and Warne, 1978; Hovis, 1966; Huang and Kerr, 1960; Hunt et al., 1950; Hussein, 1982; Keller et al., 1952; White, 1974). However, spectra in this region do not contain features directly attributable to transition metal ions such as  $\text{Fe}^{2+}$  and  $\text{Mn}^{2+}$  which are of considerable importance in studies of the deposition and diagenesis of carbonates. In addition, reflectance spectra in the VIS and NIR are more easily obtained than those in the MIR. Transmission spectra in the MIR are most readily obtained from ma-

terial which has been ground to a powder and pressed into alkali halide pellets or discs. Particles must be  $2 \mu\text{m}$  in diameter or smaller or particle size effects in both transmission and reflection spectra in the MIR cause significant variations in spectral properties which are unrelated to mineralogy or chemical composition of the samples (Estep-Barnes, 1977; Farmer and Russell, 1966; Russell, 1974; Tuddenham and Lyon, 1960). The prolonged grinding necessary to reduce samples to particle sizes of  $2 \mu\text{m}$  or less may cause serious structural damage to mineral samples, and in carbonates may alter the mineralogy (Milliman, 1974).

It is generally assumed that the particle size problems encountered in the MIR will affect spectra in the VIS and NIR, too. Data presented in this paper, however, show spectra in the VIS and NIR may be obtained from samples in any form: powders, sands, and broken, sawed, or polished rock surfaces.

In addition, the VIS and NIR are the regions of the spectrum in which reflectance data may be obtained remotely. Remotely obtained spectra in the MIR are primarily thermal emission curves, although at the shortest wavelengths ( $3\text{--}5 \mu\text{m}$ ), spectra contain both absorption and emission features superimposed (Goetz and Rowan, 1981). Thus VIS and NIR laboratory data are of particular interest because they may be directly compared to and aid in interpretation of features seen in remotely obtained data.

Thus, while transmission studies in the MIR, where the fundamental modes occur, are preferable for studies of crystal structure and solid state physics, reflectance spectra in the VIS and NIR are more suitable for many other types of geological applications.

### *Carbonate bands*

Band positions for carbonates in this spectral region reported by previous workers are given in Table 4. Data reported by Hunt and Salisbury (table III, p. 25, 1971) for carbonate band positions in calcite and dolomite spectra show the same trends found in the course of this study, i.e., that bands in dolomite spectra occur at shorter wavelengths than equivalent bands in calcite spectra. Although the positions reported by Hunt and Salisbury (1971) for bands which correspond to bands 4, 5, and 6 of this study are similar to those reported here, their reported positions for bands 1 and 2 in both calcite and dolomite spectra are at longer wavelengths than those reported in this study. This may be due to some difference in internal calibration of their instrument, or may result from the different methods used to determine band position. Or, since Hunt and Salisbury (1971) do not mention having verified the mineralogy of their samples, it may be due to the occurrence in their samples of mineral phases other than those assumed to be present.

Absolute values of band positions are less important than differences in band positions between different mineral types. In the course of this study, spectra of some samples were measured on two different instruments, the



Table 4. Band positions and assignments for calcite from the literature

	Band Position	Band Assignment
Hunt and Salisbury (1971)	2.55 $\mu\text{m}$	$\nu_1+2\nu_3$
	2.35 $\mu\text{m}$	$3\nu_3$
	2.16 $\mu\text{m}$	$\nu_1+2\nu_3+\nu_4$ or $3\nu_1+2\nu_4$
	2.00 $\mu\text{m}$	$2\nu_1+2\nu_3$
	1.90 $\mu\text{m}$	$\nu_1+3\nu_3$
Hexter (1958)	2.55 $\mu\text{m}$	$2\nu_3+270+2\times 416$
	2.37 $\mu\text{m}$	$2\nu_3+270+3\times 416$
Schroeder et al. (1962)	2.54 $\mu\text{m}$	
Matossi (1928)	2.533 $\mu\text{m}$	$2\nu_3+\nu_1$
	2.500 $\mu\text{m}$	"
	2.330 $\mu\text{m}$	$3\nu_3$
	2.300 $\mu\text{m}$	"

one described above, and an instrument which is commercially available, a Beckman DK-2A Ratio-Recording Spectroreflectometer. Both instruments gave equivalent results. However, data taken with the Beckman DK-2A consistently gives band positions which are 0.025  $\mu\text{m}$  lower than those determined by the University of Hawaii instrument (Roger Clark, Michael Gaffey, personal communication). This would indicate that comparison of precise band positions determined by different instruments cannot be made without careful interlaboratory calibrations.

The 7 bands reported here are a minimum for the number of carbonate bands in this spectral region. Hunt and Salisbury (1971) report 5 carbonate bands in this region. However, Hexter (1958), Hunt and Salisbury (1971) and Schroeder et al. (1962) all noted that the two strong bands near 2.3 and/or 2.5  $\mu\text{m}$  are asymmetric with a shoulder on the short-wavelength side. In this study the shoulder on the band in the 2.3  $\mu\text{m}$  region has been resolved as band 3. It was not possible to fit the 2.5  $\mu\text{m}$  feature as two bands using the GFIT program, so that feature was fit as one band. The absence of this extra band in the fits results in the differences between the fit curve and the data seen in the 2.5  $\mu\text{m}$  region in Figure 2. George Rossman (pers. comm.) found that a high resolution transmission spectrum of a single calcite crystal showed, in addition to the strong features discussed here, several weak features near 2.402, 2.114, 1.965, 1.845  $\mu\text{m}$ , and resolved band 7 into two bands at 1.758 and 1.732  $\mu\text{m}$ . Plots such as Figure 3 indicate there are additional weak absorption features at wavelengths shorter than 1.6  $\mu\text{m}$ , although the low spectral resolution of these data precluded gaussian anal-

ysis. Thus there are several weak carbonate bands in this region in addition to the strong absorption features discussed in this study.

Absorptions in the VIS and NIR are overtones and combination tones of fundamental internal and lattice vibrations which occur in the MIR and FIR. Exact causes of differences in carbonate band positions between spectra of different mineral types must be related to differences in positions of these fundamental modes. Data on fundamental internal and lattice modes for carbonate minerals have been reported by a number of workers (e.g., Adler and Kerr, 1962, 1963a,b; Chester and Elderfield, 1966, 1967; Denisov et al., 1982; Frech et al., 1980; Farmer and Warne, 1978). Assignments for vibrational modes in the NIR given in the literature are listed in Table 4. However, as can be seen from Table 4, there is no agreement on the assignments for these bands in the NIR. More complex models than those used to calculate the assignments given in Table 4 have been used to explain 2-phonon absorptions in the MIR. Work by Hellwege et al. (1970), Schroeder et al. (1962) and others indicates that the best data for making band assignments and testing theories of lattice dynamics are obtained by making low-temperature measurements on oriented single crystals, a procedure too cumbersome and time-consuming for routine petrographic work. New band assignments have not been attempted here because the purpose of this work was to investigate the use of reflectance spectroscopy as a routine tool for mineralogical and petrographic work, rather than to apply it to studies in solid state physics. Thus measurements were made at room temperatures on material in a variety of forms.

#### *Fe<sup>2+</sup> bands*

Figure 14 shows that while Fe<sup>2+</sup> in calcites and dolomites produces a broad double absorption band in their spectra near 1.2  $\mu\text{m}$ , the exact shapes and positions of these bands are not the same for the two minerals. Cations in dolomites and calcites are surrounded by six oxygens forming an octahedron which is slightly elongated in the direction of the c-axis (Lippmann, 1973; Effenberger et al., 1981). Burns (1970) states that the energy of an absorption is inversely proportional to the fifth power of the metal ligand distance. The metal-ligand distance in calcite is larger than that in the B-site (generally considered to be the site occupied by Fe<sup>2+</sup>) in dolomites (Reeder, 1983). This difference is reflected in the fact that the Fe<sup>2+</sup> absorption in the dolomite spectrum occurs at shorter wavelengths (higher energies) than the Fe<sup>2+</sup> band in the calcite spectrum.

Crystal field theory predicts that a 3d<sup>6</sup> ion in an octahedral site will produce a single absorption due to a Laporte forbidden transition from <sup>5</sup>T<sub>2g</sub>(t<sub>2g</sub>)<sup>4</sup>(e<sub>g</sub>)<sup>2</sup> to <sup>5</sup>E<sub>g</sub>(t<sub>2g</sub>)<sup>3</sup>(e<sub>g</sub>)<sup>3</sup> (Ballhausen, 1962; Burns, 1970). Distortion of the octahedral site leads to lifting of the degeneracies of the d-orbitals, and two or more absorption bands may occur (Burns, 1970). The distortion of the cation site in calcite is greater than that of the B-site in dolomite, as shown by its qua-

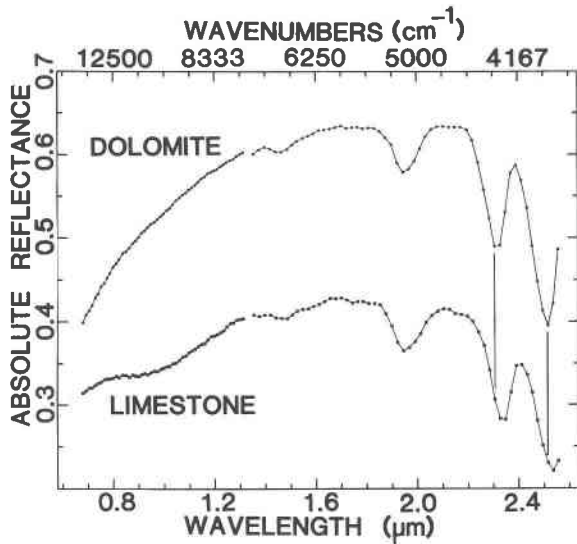


Fig. 15. Spectra of dolomite and limestone from the Mississippian Lodgepole Formation in central Montana. The asymmetric feature near  $1.9 \mu\text{m}$  is due to water in fluid inclusions and masks the carbonate bands in this region of the spectrum. However, the two carbonate bands near  $2.3$  and  $2.5 \mu\text{m}$  make it possible to distinguish dolomite from calcite. Vertical lines indicate equivalent channels in the two spectra. Dots—data points, lines connect data points to outline bands.

dratic elongation (Reeder, 1983). The  $\text{Fe}^{2+}$  band in the calcite spectrum shows more pronounced doubling (greater splitting) than that in the dolomite spectrum, reflecting this difference. This implies that the permanent distortion of the cation site must play an important part in removing the degeneracies of the  $d$ -orbitals.

#### Absorption edge

The absorption edge into the UV extends to longer wavelengths in spectra of dolomites and aragonites than in spectra of calcites. The high energy of this feature indicates that it is probably a charge transfer band. The position of this absorption edge varies with variations in chemical composition as well, shifting to longer wavelengths in dolomite spectra with increasing iron content (see Figs. 13 and 14).

#### Mineralogical applications

Positions of the carbonate bands are diagnostic of mineralogy. The presence of iron bands, and their shapes and positions can also aid in identification of the calcite group minerals.

Band-band plots shown in Figures 9, 10 and 11 are a convenient way to display the data listed in Table 2 and discussed above. These plots are particularly helpful because precise band positions determined by different workers may vary due to differences between instruments and lack of interlaboratory calibrations. However, the patterns of relative band positions shown in these plots should remain the same, regardless of the instrument used. In

Figure 9 aragonites and calcites fall together in one group, while the dolomites cluster in a second. In Figures 10 and 11, all three minerals cluster into separate groups. Thus while dolomites may be separated from calcite and aragonite on the basis of the positions of bands 1 and 2 alone, bands 2, 3, and 4 are more useful in distinguishing aragonite from calcite.

Figure 12 shows band width may also be a useful parameter in mineral identification. Again the three minerals can be separated into three distinct groups on the basis of band width.

As described above, positions of bands 5 through 7 also vary with mineral type. However, even small amounts of water present as fluid inclusions can cause apparent shifts in the positions of these bands. Or if the water bands are strong enough they may dominate the spectrum in the  $1.9 \mu\text{m}$  region and mask carbonate bands 5 and 6 entirely, so that a single feature near  $1.9 \mu\text{m}$  is seen. This is a problem of particular concern in remote sensing, where spectra of whole rocks, rather than individual mineral specimens, will be obtained, and where absorptions due to atmospheric water may preclude taking data in this region. The two minerals most abundant in ancient rocks, however, are calcite and dolomite (Pettijohn, 1975). The four bands in the  $2.0$  and  $2.5 \mu\text{m}$  region are relatively unaffected by amounts of fluid inclusions which this study indicates are common, and data presented above show these four bands are sufficient for distinguishing between these two minerals.

An example of this is shown in Figure 15. This figure shows spectra of a dolomite and a limestone from the Mississippian Lodgepole Formation in central Montana. Although water bands mask the carbonate bands in the  $1.9 \mu\text{m}$  region, the positions of the strong  $2.3$  and  $2.5 \mu\text{m}$  bands can be used to distinguish the two samples, even without the aid of gaussian analysis. Additional features in these spectra include a weak band near  $1.4 \mu\text{m}$  which is also due to water (Hunt and Salisbury, 1971). The limestone spectrum contains a weak  $\text{Fe}^{2+}$  band near  $1.3 \mu\text{m}$ . Absorption bands at shorter wavelengths are probably due to  $\text{Fe}^{3+}$  in iron oxides (Singer, 1981, 1982) formed by weathering of pyrite (Jenks, 1972). The dolomite spectrum shows no  $\text{Fe}^{3+}$  bands, but does have a smooth drop-off at shorter wavelengths, the origin of which is not understood at present.

The broad double absorption band near  $1.2 \mu\text{m}$  in carbonate spectra not only indicates the presence of  $\text{Fe}^{2+}$ , but can aid in mineral identification as well. Although substitution of  $\text{Fe}^{2+}$  in aragonites is extremely limited (Speer, 1983), the absence of an iron band does not necessarily indicate the sample belongs to the aragonite group, as non-ferroan calcites and dolomites are common. However, the presence of an  $\text{Fe}^{2+}$  band is indicative of a calcite group mineral. The shape and position of the band can aid in distinguishing between calcite and dolomite as the  $\text{Fe}^{2+}$  band in calcite spectra occurs at longer wavelengths and shows more pronounced doubling than the  $\text{Fe}^{2+}$  band in dolomite spectra.

### Conclusions

Reflectance spectroscopy in the visible (VIS) and near infrared (NIR) (0.35 to 2.55  $\mu\text{m}$ ) offers a rapid, nondestructive technique for determination of mineralogy of common carbonate minerals, and provides a useful complement to existing petrographic and mineralogical techniques for studying carbonates. The following may be concluded about reflectance spectra of these minerals as a result of this study:

1. Reflectance spectra of aragonite, calcite, and dolomite all contain at least 7 absorption bands in the 1.60 to 2.55  $\mu\text{m}$  region caused by vibrations of the carbonate radical.

2. Positions and widths of these 7 bands are diagnostic of mineralogy. Carbonate bands in spectra of dolomites occur at shorter wavelengths than equivalent bands in calcite spectra. Increasing  $\text{Fe}^{2+}$  content in dolomites causes the carbonate bands in their spectra to shift to longer wavelengths. Carbonate bands in spectra of aragonites may occur at the same, longer, or shorter wavelengths than equivalent bands in calcite spectra, depending on the specific spectral band.

3. Although water in the form of fluid inclusions may preclude use of the weaker bands in the 1.6 to 2.0  $\mu\text{m}$  region, if the water content is low the 4 bands centered in the 2.00 to 2.55  $\mu\text{m}$  region are sufficient for discrimination between these three carbonate minerals.

4. Absolute intensities of carbonate bands and brightness of spectra are a function of particle size and packing and do not reflect mineralogical differences. Relative intensities, shapes, and positions of bands within a spectrum, however, are not significantly affected by variations in grain size or packing.

5. Because solid substitution of  $\text{Fe}^{2+}$  into aragonite group minerals is extremely limited (Deer et al., 1962; Speer, 1983), presence of absorption features due to  $\text{Fe}^{2+}$  in spectra indicates minerals are members of the calcite group rather than the aragonite group.

6. Shape and position of  $\text{Fe}^{2+}$  bands, when present, may help determine mineralogy.  $\text{Fe}^{2+}$  bands in ferroan calcite spectra are centered at longer wavelengths (1.3  $\mu\text{m}$ ) and show more pronounced doubling than those in spectra of ferroan dolomites, which are centered near 1.2  $\mu\text{m}$ .

7. Spectra may be obtained from rock and mineral samples in any form: whole rocks, sands, or powders.

### Acknowledgments

I would like to thank Robert Huguenin who first suggested this project and who provided many of the samples that were used. Thanks for supplying mineral samples also go to the Smithsonian, the British Museum, and George McCormick at the University of Iowa. I want to express my appreciation to John Adams at the University of Washington for the use of his spectrophotometer. I would like to thank Edith Jenks and Michael Gaffey for their assistance in the field. X-ray fluorescence analyses were provided by John Sinton at the University of Hawaii. Kevin Reed performed the AA analyses and assisted with the X-ray diffraction work. I would like to thank George Rossman and an unnamed reviewer for their critical reviews of the manuscript. Funding for this work was provided by Jet Propulsion Laboratory

Grant #JPL 956370 and by Gaylord, Leonard, and Edna Cobeen. This is Planetary Geosciences Division Publication Number 400.

### References

- Adams, J. B. (1974) Visible and near-infrared diffuse reflectance spectra of pyroxenes as applied to remote sensing of solid objects in the solar system. *Journal of Geophysical Research*, 79, 4829–4836.
- Adler, H. H. and Kerr, P. F. (1962) Infrared study of aragonite and calcite. *American Mineralogist*, 47, 700–717.
- Adler, H. H. and Kerr, P. F. (1963a) Infrared absorption frequency trends for anhydrous normal carbonates. *American Mineralogist*, 48, 124–137.
- Adler, H. H. and Kerr, P. F. (1963b) Infrared spectra, symmetry and structure relations of some carbonate minerals. *American Mineralogist*, 48, 839–853.
- Aines, R. D. and Rossman, G. R. (1984) Water in minerals? A peak in the infrared. *Journal of Geophysical Research*, 89, B6, 4059–4071.
- Ballhausen, C. J. (1962) *Introduction to Ligand Field Theory*. McGraw-Hill Book Company, New York.
- Bjerrum, J., Ballhausen, C. J., and Jorgensen, C. K. (1954) Studies on absorption spectra I. Results of calculations on the spectra and configuration of copper(II) ions. *Acta Chemica Scandinavica*, 8, 1275–1289.
- Burns, R. G. (1970) *Mineralogical Applications of Crystal Field Theory*. Cambridge University Press, London.
- Chester, R. and Elderfield, H. (1966) The infra-red determination of total carbonate in marine sediments. *Chemical Geology*, 1, 277–290.
- Chester, R. and Elderfield, H. (1967) The application of infrared absorption spectroscopy to carbonate mineralogy. *Sedimentology*, 9, 5–21.
- Clark, R. N. (1980) A large-scale interactive one dimensional array processing system. *Publications of the Astronomical Society of the Pacific*, 92, 221–224.
- Clark, R. N. (1981a) The spectral reflectance of water–mineral mixtures at low temperatures. *Journal of Geophysical Research*, 86, B4, 3074–3086.
- Clark, R. N. (1981b) Water frost and ice: the near-infrared spectral reflectance 0.65–2.5  $\mu\text{m}$ . *Journal of Geophysical Research*, 86, B4, 3087–3096.
- Clark, R. N. and Roush, T. L. (1984) Reflectance spectroscopy: quantitative analysis techniques for remote sensing applications. *Journal of Geophysical Research*, 89, B7, 6329–6340.
- Deer, W. A., Howie, R. A., and Zussman, J. (1962) *Rock-Forming Minerals*, Vol. 5. Non-Silicates. Longman Group, London.
- Denisov, V. N., Mavrin, B. N., Podobedov, V. B., and Sterin, Kh. E. (1982) Hyper-Raman scattering by phonons and mixed polaritons in a calcite crystal. *Physica Status Solidi (B)*, 110, 183–189.
- Dowty, E. and Clark, J. R. (1973) Crystal structure refinement and optical properties of a  $\text{Ti}^{3+}$  fassaite from the Allende meteorite. *American Mineralogist*, 58, 230–242.
- Effenger, H., Mereiter, K., and Zemmann, J. (1981) Crystal structure refinements of magnesite, calcite, rhodochrosite, siderite, smithonite, and dolomite, with discussion of some aspects of the stereochemistry of calcite type carbonates. *Zeitschrift für Kristallographie*, 156, 233–243.
- Estep-Barnes, P. A. (1977) Infrared spectroscopy. In J. Zussman, Ed., *Physical Methods in Determinative Mineralogy*, Second Edition, p. 529–603. Academic Press, New York.
- Farmer, V. C. and Russell, J. D. (1966) Effects of particle size and structure on the vibrational frequencies of layer silicates. *Spectrochimica Acta*, 22, 389–398.
- Farmer, V. C. and Warne, S. St. J. (1978) Infrared spectroscopic evaluation of iron contents and excess calcium in minerals of the dolomite–ankerite series. *American Mineralogist*, 63, 779–781.
- Farr, T. G., Bates, B. A., Ralph, R. L., and Adams, J. B. (1980)

- Effects of overlapping optical absorption bands of pyroxene and glass on the reflectance spectra of lunar soils. In R. B. Merrill, Ed., Proceedings of the Eleventh Lunar and Planetary Sciences Conference, 1, p. 719–729. Pergamon Press, New York.
- Frech, R., Wang, E. C., and Bates, J. B. (1980) The i.r. and Raman spectra of CaCO<sub>3</sub> (aragonite). *Spectrochimica Acta*, 36A, 915–919.
- Gaffey, S. J. (1985) Reflectance spectroscopy in the visible and near-infrared (0.35–2.55  $\mu\text{m}$ ): applications in carbonate petrology. *Geology*, 13, 270–273.
- Gatehouse, B. M., Livingston, S. E., and Nyholm, R. S. (1958) The infrared spectra of some simple and complex carbonates. *Journal of the Chemical Society of London*, 1958, III, 3137–3142.
- Goetz, A. F. H. and Rowan, L. C. (1981) Geologic remote sensing. *Science*, 211, 781–791.
- Goldsmith, J. R. (1983) Phase relations of rhombohedral carbonates. In R. J. Reeder, Ed., Carbonates: Mineralogy and Chemistry, Mineralogical Society of America Reviews in Mineralogy Volume 11, p. 49–76. Mineralogical Society of America.
- Hellwege, K. H., Lesch, W., Plihal, M., and Schaack, G. (1970) Zwei-Phononen-Absorptionsspektren und Dispersion der Schwingungsweige in Kristallen der Kalkspatstruktur. *Zeitschrift für Physik*, 232, 61–86.
- Hexter, R. M. (1958) High-resolution, temperature-dependent spectra of calcite. *Spectrochimica Acta*, 10, 281–290.
- Hexter, R. M. and Dows, D. A. (1956) Low-frequency librations and the vibrational spectra of molecular crystals. *Journal of Chemical Physics*, 25, 504–509.
- Holmes, O. G. and McClure, D. S. (1957) Optical spectra of hydrated ions of the transition metals. *Journal of Chemical Physics*, 26, 1686–1694.
- Hovis, W. A., Jr. (1966) Infrared spectral reflectance of some common minerals. *Applied Optics*, 5, 245–248.
- Huang, C. K. and Kerr, P. F. (1960) Infrared study of the carbonate minerals. *American Mineralogist*, 45, 311–324.
- Hunt, G. R. (1977) Spectral signatures of particulate minerals in the visible and near-infrared. *Geophysics*, 42, 501–513.
- Hunt, G. R. and Salisbury, J. W. (1971) Visible and near-infrared spectra of minerals and rocks: II. Carbonates. *Modern Geology*, 2, 23–30.
- Hunt, J. M., Wisherd, M. P., and Bonham, L. C. (1950) Infrared absorption spectra of minerals and other inorganic compounds. *Analytical Chemistry*, 22, 1478–1497.
- Hussein, S. A. (1982) Infrared spectra of some Egyptian sedimentary rocks and minerals. *Modern Geology*, 8, 95–105.
- Jenks, S. (1972) Environment of deposition and diagenesis of the Lodgepole Formation (Mississippian), central Montana. Montana Geological Survey 21st Annual Field Conference Guidebook, 19–28.
- Kaper, H. G., Smits, D. W., Schwarz, U., Takakubo, K., and Van Woerden, H. (1966) Computer analysis of observed distributions into gaussian components. *Bulletin of the Astronomical Institute of the Netherlands*, 18, 465–487.
- Keller, W. D., Spotts, J. H., and Biggs, D. L. (1952) Infrared spectra of some rock-forming minerals. *American Journal of Science*, 250, 453–471.
- Lippmann, F. (1973) *Sedimentary Carbonate Minerals*. Springer-Verlag, New York.
- Matossi, Frank (1928) Absorption linear polarisierter ultraroter Strahlung im Kalkspat ( $2\mu$ – $16\mu$ ). *Zeitschrift für Physik*, 48, 616–623.
- McCord, T. B., Clark, R. N., Hawke, B. R., McFadden, L. A., Owensby, P. D., Pieters, C. M., and Adams, J. B. (1981) Moon: near-infrared spectral reflectance, a first good look. *Journal of Geophysical Research*, 86, B11, 10883–10892.
- Milliman, J. D. (1974) *Marine Carbonates*. Springer-Verlag, New York.
- Norrish, K. and Hutton, J. T. (1969) An accurate X-ray spectrographic method for the analysis of a wide range of geologic samples. *Geochimica et Cosmochimica Acta*, 33, 431–451.
- Pettijohn, F. J. (1975) *Sedimentary Rocks*, Third Edition. Harper and Row, New York.
- Reeder, R. J. (1983) Crystal chemistry of the rhombohedral carbonates. In R. J. Reeder, Ed., Carbonates: Mineralogy and Chemistry, Mineralogical Society of America Reviews in Mineralogy Volume 11, p. 1–47. Mineralogical Society of America.
- Russell, J. D. (1974) Instrumentation and techniques. In V. C. Farmer, Ed., *The Infrared Spectra of Minerals*, Mineralogical Society Monograph 4, p. 11–25. The Mineralogical Society, London.
- Scheetz, B. E. and White, W. B. (1977) Vibrational spectra of the alkaline earth double carbonates. *American Mineralogist*, 62, 36–50.
- Schroeder, R. A., Weir, C. E., and Lippencott, E. R. (1962) Lattice frequencies and rotational barriers for inorganic carbonates and nitrates from low temperature infrared spectroscopy. *Journal of Research of the National Bureau of Standards A. Physics and Chemistry*, 66a, 407–434.
- Singer, R. B. (1981) Near-infrared spectral reflectance of mineral mixtures: systematic combinations of pyroxenes, olivines, and iron oxides. *Journal of Geophysical Research*, 86, B9, 7967–7982.
- Singer, R. B. (1982) Spectral evidence for the mineralogy of high-albedo soils and dust on Mars. *Journal of Geophysical Research*, 87, B12, 10159–10168.
- Speer, J. A. (1983) Crystal chemistry and phase relations of orthorhombic carbonates. In R. J. Reeder, Ed., Carbonates: Mineralogy and Chemistry, Mineralogical Society of America Reviews in Mineralogy Volume 11, p. 145–190. Mineralogical Society of America.
- Tuddenham, W. M. and Lyon, R. J. P. (1960) Infrared techniques in the identification and measurement of minerals. *Analytical Chemistry*, 32, 1630–1634.
- Venable, W. H., Jr., Weidner, V. R., and Hsia, J. J. (1976) Information sheet on optical properties of pressed Halon coatings, Report, National Bureau of Standards, Washington, D.C.
- Weidner, V. R. and Hsia, J. J. (1981) Reflection properties of pressed polytetrafluoroethylene powder. *Journal of the Optical Society of America*, 71, 856–861.
- Weir, C. E. and Lippincott, E. R. (1961) Infrared studies of aragonite, calcite, and vaterite type structures in the borates, carbonates, and nitrates. *Journal of Research of the National Bureau of Standards A. Physics and Chemistry*, 65, 173–183.
- Wendlandt, W. W. and Hecht, H. G. (1966) *Reflectance Spectroscopy*. John Wiley and Sons, Interscience Publishers, New York.
- White, W. B. (1974) The carbonate minerals. In V. C. Farmer, Ed., *The Infrared Spectra of Minerals*, Mineralogical Society Monograph 4, p. 227–284. Mineralogical Society, London.

*Manuscript received, February 7, 1984;  
accepted for publication, September 16, 1985.*